Self-assembly, thermal stability and photoluminescence of two mixed-ligand silver(I) networks *via* 2D → 2D and 2D → 3D parallel interpenetration of (4,4) nets†

Di Sun,[a] Qin-Juan Xu,[a] Chun-Yin Ma,[a] Na Zhang,[a] Rong-Bin Huang*[a] and Lan-Sun Zheng[ab]

Received 23rd March 2010, Accepted 14th May 2010
DOI: 10.1039/c0ce00017e

Two mixed-ligand silver(I) coordination polymers (CPs) $[Ag_2(dmapym)_2(suc)\cdot H_2O]_n$ (**1**) and $[Ag_2(dmapym)_2(bdc)\cdot 2H_2O]_n$ (**2**), (dmapym = 2-amino-4,6-dimethylpyrimidine, H_2suc = succinic acid, H_2bdc = 1,3-benzenedicarboxylic acid), were synthesized and characterized. The structure of **1** presents an argentophilic interaction enhanced 2-crossing [2]-catenane motif formed between pairs of parallel interpenetrating 2D 4^4-**sql** nets. For **2**, as the dicarboxylate changes from flexible H_2suc to rigid V-shaped H_2bdc, each highly undulated 2D 4^4-**sql** net was penetrated in parallel by the two nearest neighbouring ones and thus the overall 2D → 3D network is formed. The geometries and flexibility of dicarboxylates influence the coordination environments of metal ions and arrangement of ligands and thus determine the structures of the CPs. The photoluminescent and thermal properties of **1** and **2** have also been investigated.

1. Introduction

The current interest in polymeric coordination networks is dramatically expanding not only because of their potential properties as functional solid materials, in host–guest chemistry, ion exchange, catalysis, and for the development of optical, magnetic and electronic devices, but also due to their intriguing variety of architectures and topologies.[1] Infinite entangled structures, such as interpenetration, polycatenation, polythreading and Borromean structures, are the subject of intensive current research[2] and have been well discussed in comprehensive reviews.[3] As we know, not only can interdigitation of adjacent sheets, interpenetration of the sheets, and intercalation of guests,[4] minimize void efficiently, but also aid from non-covalent inteactions such as Ag···Ag interaction is important.[5] With specific regard to 2D networks, despite the fact that 2- and 4-crossing [2]-catenane motifs constructed through the 2D → 2D parallel interpenetration of pairs of 4^4-**sql** nets have been recognized,[6] argentophilic interaction enhanced interpenetrating 2D nets are still rare. On the other hand, a dimensionality increase from 2D layers to an overall 3D network can also occur in the case of parallel interpenetration, although such 2D → 3D dimensional expansion is relatively limited.[3] Since the publication of the first example in 1997,[7] a series of 2D → 3D interpenetrating coordination polymers (CPs) have been obtained.[8] The 4^4-**sql** net is one of the most common topologies in 2D CPs, which are inclined to interpenetrate when a large four-membered ring is formed and this net usually shows undulated features. Usually, it is widely acknowledged that long spacer ligands favor the formation of interpenetrated motifs, however, using mixed simple ligands with metal ions to construct complicated motifs is still rare. During our recent studies, in order to search for a new class of topological structures in Ag(I)/aminopyrimidyl derivatives/dicarboxylate system,[9] we surprisingly obtained two parallel interpenetrating 2D → 2D and 2D → 3D mixed-ligand silver(I) CPs, namely $[Ag_2(dmapym)_2(suc)\cdot H_2O]_n$ (**1**) and $[Ag_2(dmapym)_2(bdc)\cdot 2H_2O]_n$ (**2**), (dmapym = 2-amino-4,6-dimethylpyrimidine, H_2suc = succinic acid, H_2bdc = 1,3-benzenedicarboxylic acid).

2. Experimental

2.1. Materials and methods

All chemicals and solvents used in the syntheses were of analytical grade and used without further purification. IR spectra were measured on a Nicolet 740 FTIR Spectrometer in the range of 4000–400 cm^{-1}. Elemental analyses were carried out on a CE instruments EA 1110 elemental analyzer. Photoluminescent properties were measured on a Hitachi F-4500 Fluorescence Spectrophotometer. TGA was measured from 20 to 800 °C on a SDT Q600 instrument at a heating rate 5 °C min^{-1} under the N_2 atmosphere (100 ml min^{-1}). X-Ray powder diffractions were measured on a Panalytical X-Pert pro diffractometer with Cu-Kα radiation.

2.2. Syntheses

2.2.1. $[Ag_2(dmapym)_2(suc)\cdot H_2O]_n$ (1). Reaction of $AgNO_3$ (167 mg, 1 mmol), dmapym (123 mg, 1 mmol) and H_2suc (118 mg, 1mmol) took place in methanol–H_2O media (15 ml, v/v = 2 : 1) in the presence of ammonia (25%, 0.5 mL) in air under ultrasonic treatment (160W, 40 KHz, 20 min) at 50 °C.

[a]*Department of Chemistry, College of Chemistry and Chemical Engineering, Xiamen University, Xiamen, 361005, People's Republic of China*
[b]*State key Laboratory for Physical Chemistry of Solid Surfaces, Xiamen University, Xiamen, 361005, People's Republic of China. E-mail: rbhuang@xmu.edu.cn*

† Electronic supplementary information (ESI) available: X-ray powder diffraction patterns of the compounds. CCDC reference numbers 769616 and 769617 are for **1** and **2**, respectively. For ESI and crystallographic data in CIF or other electronic format see DOI: 10.1039/c0ce00017e

The resultant colorless solution (pH = 9.25) was allowed slowly to evaporate at room temperature for one week to give colorless block crystals of **1**. The crystals were isolated by filtration and washed by deionized water and dried in air. Yield: *ca.* 82% based on Ag. Elemental analysis: Anal. Calc. for $Ag_2C_{16}H_{23}N_6O_5$: C 32.29, H 3.90, N 14.12%. Found: C 32.33, H 3.85, N 14.08%. Selected IR peaks (cm^{-1}): 3424 (s), 3331(s), 3169(m), 1668(m), 1574(s), 1487(w), 1399(w), 1225(w), 1032(w), 807(w), 652(w), 552(w), 502(w).

2.2.2. $[Ag_2(dmapym)_2(bdc)\cdot 2H_2O]_n$ (2). Synthesis of **2** was similar to that of **1**, but with H_2bdc (166 mg, 1 mmol) instead of H_2suc. Colorless crystals of **2** were grown from the filtrate (pH = 9.58) in 68% yield based on Ag. Elemental analysis: Anal. Calc. For $Ag_2C_{20}H_{26}N_6O_6$: C 36.28, H 3.96, N 12.69%. Found: C 36.35, H. 3.88, N 12.76%. Selected IR peaks (cm^{-1}): 3418 (s), 3318(s), 3157(m), 1661(m), 1562(s), 1481(w), 1381(w), 1225(w), 733(w), 552(w), 552(w), 508(w).

2.3. X-Ray crystallography

Single crystals of the complexes **1** and **2** with appropriate dimensions were mounted on a glass fiber and used for data collection. Data were collected on a Rigaku R-AXIS RAPID Imaging Plate single-crystal diffractometer equipped with a graphite-monochromated Mo-Kα radiation source (λ = 0.71073 Å) in ω scan mode for **1** and **2**. The crystal structures were solved by direct methods and refined with the full-matrix least-squares technique on F^2 using the SHELXS-97 and SHEXL-97 programs.[10] All non-hydrogen atoms were refined with anisotropic thermal parameters. The positions of the water H atoms were assigned to calculated positions with isotropic thermal parameters and refined with the O–H bond length restrained to 0.85 Å. The crystallographic details of **1** and **2** are summarized in Table 1. Selected bond lengths and angles for **1** and **2** are collected in Table 2. The hydrogen bond geometries for **1** and **2** are shown in Table 3.

Table 1 Crystal data for **1** and **2**[a]

Complex	**1**	**2**
Formula	$Ag_2C_{16}H_{23}N_6O_5$	$Ag_2C_{20}H_{26}N_6O_6$
M_r	595.14	662.21
Crystal System	Monoclinic	Monoclinic
Space group	*C*2/*c*	$P2_1/n$
a/Å	12.502(3)	11.699(2)
b/Å	20.211(4)	11.427(2)
c/Å	9.1833(18)	18.680(4)
β (°)	112.49(3)	108.18(3)
V/Å^3	2143.9(8)	2372.7(8)
T/K	298(2)	298(2)
Z, D_c/g cm^{-3}	4, 1.844	4, 1.854
F(000)	1180	1320
μ/mm^{-1}	1.865	1.699
Ref. collected/unique	7739/1175	13894/3403
R_{int}	0.0862	0.0489
Parameters	135	312
Final *R* indices[a] [$I > 2\sigma(I)$]	$R_1 = 0.0593$	$R_1 = 0.0353$
	$wR_2 = 0.1264$	$wR_2 = 0.0778$
R indices (all data)	$R_1 = 0.0973$	$R_1 = 0.0555$
	$wR_2 = 0.1417$	$wR_2 = 0.0858$
Goodness of fit on F^2	0.996	0.999

[a] $R_1 = \sum| |F_o| - |F_c| |/\sum|F_o|$, $wR_2 = [\sum w(F_o^2 - F_c^2)^2]/\sum w(F_o 2)2]^{1/2}$.

Table 2 Selected bond lengths (Å) and angles (°) for **1** and **2**

Complex **1**[a]

Ag1–O1	2.248(5)	Ag2–N3^{iii}	2.189(6)
Ag1–N2^{i}	2.503(6)	Ag2–O2^{iv}	2.755(5)
Ag1–Ag2^{ii}	3.2770(16)		
O1–Ag1–O1^{i}	145.0(3)	O1^{i}–Ag1–Ag2^{ii}	72.52(15)
O1–Ag1–N2	107.4(2)	N2–Ag1–Ag2^{ii}	127.44(14)
N2–Ag1–N2^{i}	105.1(3)	N3^{iii}–Ag2–N3	160.6(3)
O1–Ag1–N2^{i}	93.78(19)	N3^{iii}–Ag2–O2^{ii}	87.05(19)
O2^{ii}–Ag2–O2^{iv}	130.5(3)	N3–Ag2–O2^{ii}	101.1(2)
N3^{iii}–Ag2–Ag1^{ii}	99.70(16)	N3–Ag2–O2^{iv}	87.05(19)

[a] Symmetry codes: (i) $-x + 1, y, -z + 3/2$; (ii) $-x + 1/2, -y + 1/2, -z + 1$; (iii) $-x, y, -z + 1/2$; (iv) $x - 1/2, -y + 1/2, z - 1/2$.

Complex **2**[b]

Ag1–N4	2.201(3)	Ag2–O3^{i}	2.306(3)
Ag1–N1	2.205(3)	Ag2–O1	2.447(3)
Ag2–N6	2.299(3)	Ag2–N3^{ii}	2.518(3)
N4–Ag1–N1	170.86(14)	N6–Ag2–N3^{ii}	93.96(12)
N6–Ag2–O3^{i}	143.33(10)	O3^{i}–Ag2–N3^{ii}	99.80(11)
N6–Ag2–O1	113.16(10)	O1–Ag2–N3^{ii}	97.50(10)
O3^{i}–Ag2–O1	98.60(11)		

[b] Symmetry codes: (i) $x - 1/2, -y + 3/2, z - 1/2$; (ii) $x + 1, y, z$.

Table 3 The hydrogen bond geometries for **1** and **2**

Complex **1**[a]

D–H···A	D–H	H···A	D···A	D–H···A
N1–H1A···O2^{ii}	0.86	2.05	2.897(9)	171
O1W–H1WA···O2^{ii}	0.85	1.96	2.806(8)	175
N1–H1B···O1^{i}	0.86	1.96	2.814(8)	175

[a] Symmetry codes: (i) $-x + 1, y, -z + 3/2$; (ii) $-x + 1/2, -y + 1/2, -z + 1$.

Complex **2**[b]

O1W–H1WA···O2	0.85	2.07	2.916(5)	179
O1W–H1WB···O4^{v}	0.85	1.89	2.740(5)	179
O2W–H2WB···O1W	0.85	1.92	2.768(7)	178
O2W–H2WA···O2^{v}	0.85	2.03	2.881(6)	178
N2–H2A···O1^{iii}	0.86	2.07	2.925(4)	175
N2–H2B···O3^{v}	0.86	1.98	2.802(4)	161
N5–H5D···O2^{vi}	0.86	2.04	2.878(4)	163
N5–H5E···O4^{i}	0.86	2.32	3.099(4)	152

[b] Symmetry code: (i) $x - 1/2, -y + 3/2, z - 1/2$; (iii) $x - 1, y, z$; (v) $-x + 3/2, y - 1/2, -z + 3/2$; (vi) $-x + 1, -y + 1, -z + 1$

3. Result and discussion

3.1. Structure descriptions

3.1.1. $[Ag_2(dmapym)_2(suc)\cdot H_2O]_n$ (1). Complex **1** crystallizes in the monoclinic space group *C*2/*c*. As shown in Fig. 1a, the asymmetric unit of **1** contains two crystallographically independent Ag(I) ions, one dmapym ligand, one half suc and one lattice water molecule. Analysis of the local symmetry of the metal atoms and ligands showed that both Ag1 and Ag2 reside on the crystallographic *C*2 axis (site occupancy factor

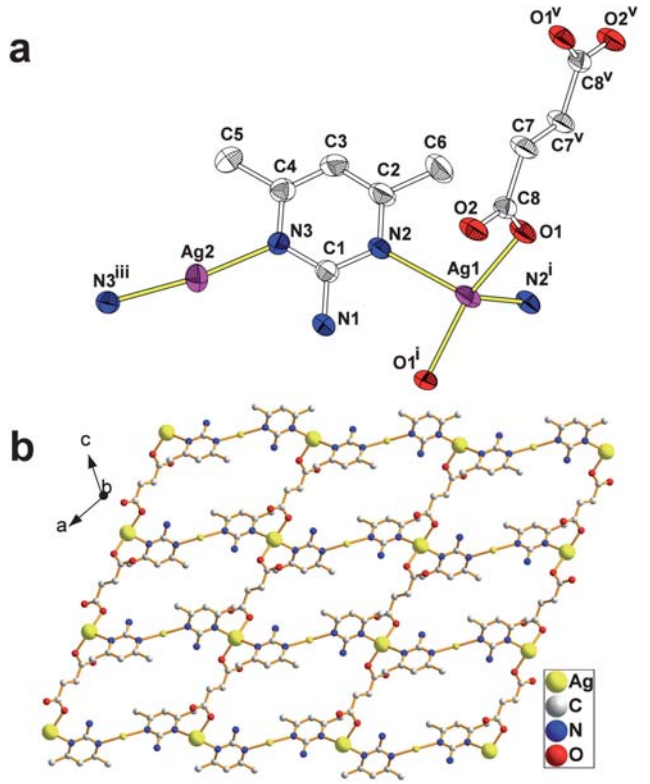

Fig. 1 (a) ORTEP plot showing the coordination environments of Ag(I) ions in **1**. Displacement ellipsoids are drawn at the 30% probability level. Lattice water molecule was omitted for clarity. Symmetry codes: (i) $-x+1$, y, $-z+3/2$; (iii) $-x$, y, $-z+1/2$; (v) $-x+3/2$, $-y+1/2$, $-z+1$. (b) A view of the undulated 4^4-**sql** net in the structure of **1**. Ag2 ions as 4-connected nodes are shown by bigger balls.

(SOF) = 1/2); the suc and water molecule are located on the inversion centers. The Ag1 is located in a distorted tetrahedron geometry and coordinated by two dmapym and two suc ligands (Ag1–O1 = 2.248(5), Ag1–N2 = 2.503(6) Å). The distortion of the tetrahedron can be indicated by the calculated value of the τ_4 parameter introduced by Houser[11] to describe the geometry of a four-coordinate metal system, which is 0.76 for Ag1 (for perfect tetrahedral geometry, $\tau_4 = 1$). The Ag2 ion, coordinated by two symmetry-related N atoms from two different dmapym ligands (Ag2–N3 = 2.189(6) Å), is located in a linear environment with an angle of 160.6(3)° which deviates from the ideal 180° due to the Ag···O weak interaction (Ag2···O2^{ii} = 2.755(5) Å; symmetry code: (ii) $-x+1/2$, $-y+1/2$, $-z+1$). Both Ag–O and Ag–N bond lengths are well-matched to those observed in similar complexes.[12] It is worthy to note that the bond length of Ag1–N2 is obviously longer than that of Ag2–N3, which may be due to the different coordination modes between Ag1 (four-coordinate) and Ag2 (two-coordinate).

In **1**, the Ag(I) ions are linked by bidentate dmapym and suc ligands to form a single 2D undulated net (Fig. 1b) incorporating an $Ag_4(dmapym)_4(suc)_2$ window of 12.36 × 9.17 Å based on the Ag···Ag distances, which is large enough to allow the insertion of a rod of another window. To better understand the structure of **1**, the topological analysis approach is employed. This net contains one type of node (Ag1 ions) and two types of linkers (dmapym and suc ligands). In **1**, tetrahedral Ag1 ions as 4-connected nodes are bridged by 2-connected dmapym and suc ligands; Ag2 ions just participate in the construction of the four-membered ring and can not be seen as nodes, so the 2D net can be simplified to be a 4^4-**sql** net.[13] The lattice water molecules are filled in the windows and hydrogen-bonded to carboxyl groups with an O_{water}–H···O_{suc} distance of 2.806(8) Å; amino groups of dmapym also interact with the carboxyl groups through N–H···O_{suc} hydrogen bonds with an average distance of 2.856(9) Å. Two kinds of hydrogen bonds determine two symmetry-related edge-sharing heteromeric rings (Fig. S1†) with a graph set $R_4^3(13)$[14] and reinforce the resultant 2D net.

A more impressive structural characteristic of complex **1** is the presence of a pair of identical 2D single nets which interpenetrate in a 2D → 2D parallel fashion, as shown in Fig. 2a. Each $Ag_4(dmapym)_4(suc)_2$ window in one net is penetrated by one suc rod of another window, and as a consequence, the windows of the network are occupied, preventing formation of the large channels. The pairs of nets interpenetrate such that 2-crossing

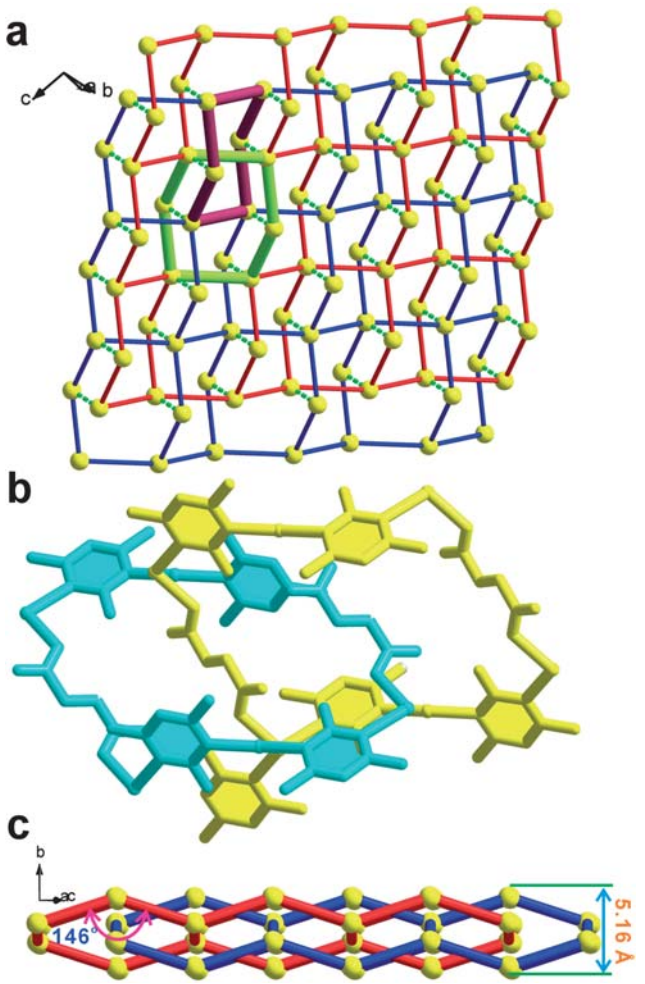

Fig. 2 (a) Schematic representation of the interpenetration of a pair of undulated 4^4-**sql** nets in **1**. The 2-crossing [2]-catenane motif is highlighted in yellow-green and purple and the Ag···Ag interactions are shown in green dashed lines. (b) Another view of the 2-crossing [2]-catenane. (c) Side view of the interpenetration of a pair of undulated 4^4-**sql** nets **1**.

[2]-catenane motifs are formed (Fig. 2b). The interpenetrating nets have parallel mean planes and are coincident, and thus an overall 2D entanglement is produced. Different from the previous documented 2D → 2D parallel interpenetrating CPs,[6b,6h] the pairs of 4^4-**sql** nets in **1** are further consolidated by Ag···Ag interactions (3.2770(16) Å) which confine the slippage of two entangled nets and combine with the interpenetration to minimize the voids between the nets. To the best of our knowledge, this is the first example of an argentophilic interaction enhanced 2D → 2D parallel interpenetrating 4^4-**sql** net, by contrast, a similar argentophilic interaction enhanced 3D interpenetrating framework was reported by Chen *et al.*[5] Alternatively, if Ag···Ag interactions in **1** are treated as connections, then the fashion of entangled pairs of nets should be considered as interpenetrated + interlocked and can be simply seen as a single, self-penetrating 2D network.

3.1.2. $[Ag_2(dmapym)_2(bdc)\cdot 2H_2O]_n$ (2). In the structure of **2**, as shown in Fig. 3a, there are two crystallographically independent Ag(I) ions, two dmapym, one bdc dianion and two lattice water molecules in an asymmetric unit. Both Ag1 and Ag2 locate in the general positions. The Ag1 is in a linear geometry completed by two N atoms from two different dmapym ligands (∠N4–Ag1–N1 = 170.86(14)°). The Ag···O weak interactions also exist around Ag1 (Ag1···O2^{vi} = 2.826(3), Ag1···O3^{v} = 2.716(3) Å; symmetry code: (v) $-x + 3/2$, $y - 1/2$, $-z + 3/2$; (vi) $-x + 1$, $-y + 1$, $-z + 1$). The Ag2 is located in a distorted tetrahedron geometry and coordinated by two dmapym and two bdc ligands with the average Ag–O and Ag–N distances of 2.377(3) and 2.409(3) Å, respectively. The τ_4 parameter is 0.73 for Ag2. Two dmapym moieties bound to Ag1 in **2** form a dihedral angle of *ca.* 67° which is much smaller than that in **1** (*ca.* 82°).

Similar to **1**, the basic structure of **2** is also a 4^4-**sql** net which is constructed by Ag2 ions, bidentate dmapym and bdc ligands (Fig. 3b). This 4^4-**sql** net also contains one type of node (four-connected Ag2 ions) and two types of linkers (two-connected dmapym and bdc ligands). Compared to the net of **1**, the net in **2** contains a larger window of 11.70 × 11.51 Å and exhibits a highly undulated character with a thickness of about 6.72 Å (Fig. 3c), as a result, each highly undulated 2D 4^4-**sql** net is simultaneously penetrated by the two nearest neighbouring ones. In other words, as shown in Fig. 4b, each window (cyan window) is simultaneously catenated by the other two (yellow and red windows). Therefore, the 2D → 3D dimensional increase can be regarded as being caused by polycatenation of the nets. Different from **1**, although the interpenetrating nets in **2** also have parallel

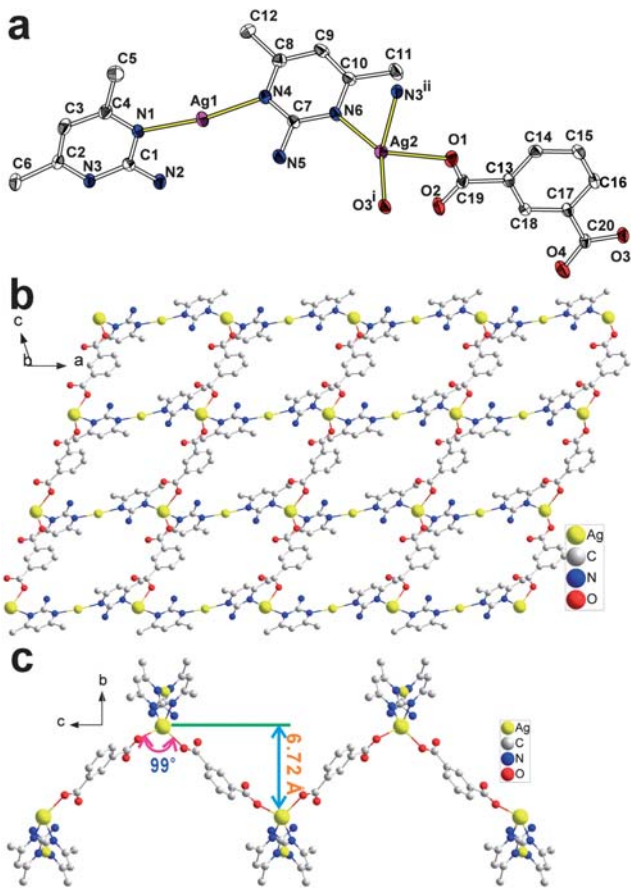

Fig. 3 (a) ORTEP plot showing the coordination environments of Ag(I) ions in **2**. Displacement ellipsoids are drawn at the 30% probability level. Lattice water molecules were omitted for clarity. Symmetry codes: (i) $x - 1/2$, $-y + 3/2$, $z - 1/2$; (ii) $x + 1$, y, z. (b) A view of the single undulated 4^4-**sql** net in the structure of **2**. Ag1 ions as 4-connected nodes are shown as bigger balls. (c) Side view of the single undulated 4^4-**sql** nets in the structure of **2**.

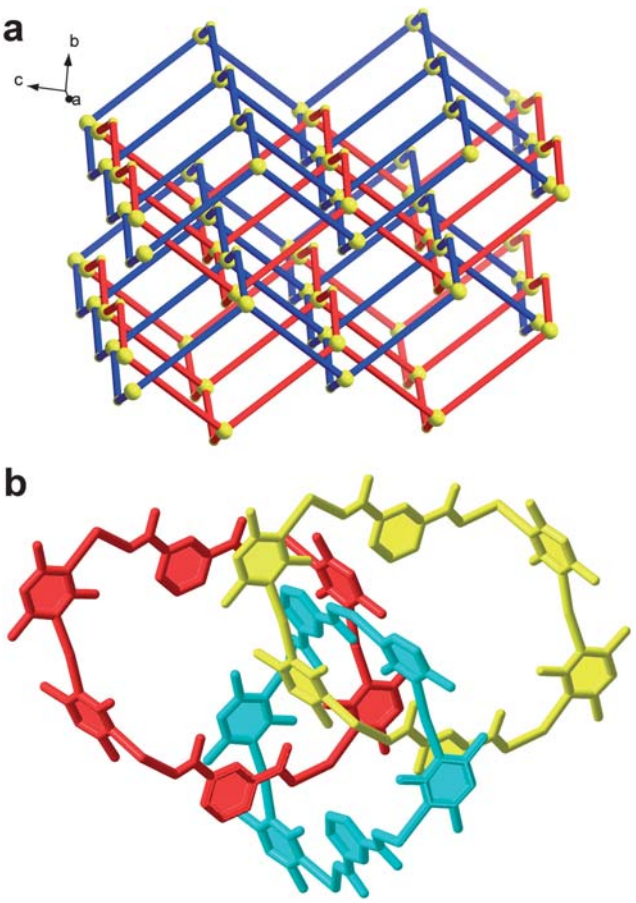

Fig. 4 (a) A view of the 2D → 3D interpenetrating undulated 4^4-**sql** net in the structure of **2**. (b) A view of catenation of windows.

mean planes, these mean planes are not coincident but are offset, and thus an overall 3D entanglement is formed (Fig. 4a). The high degree of entanglement is due to: (i) the large enough windows of the net; (ii) the highly undulated nature of the single 4^4-**sql** net.

There are abundant supramolecular interactions between adjacent nets. Lattice water molecules are filled in the voids between nets through O–H···O hydrogen bonds with an average O–H···O distance of 2.826(6) Å. Amino groups are hydrogen bonded to carboxyl groups with the N–H···O distance in the range of 2.802(4)–3.099(4) Å and combine with the water molecules to form a $R_4^4(8)$ hydrogen bond motif. The C–H···π interaction [C12–H12B···*Cg*1^{v}: $d_{H\cdots Cg}$ = 2.85 Å, $d_{C\cdots Cg}$ = 3.624(5) Å and θ = 138°; *Cg*1 is the centroid of ring C13–C18; θ is the angle of C···H···*Cg*, Fig. S2†], face-to-face π···π interaction [*Cg*1···*Cg*2^{vi} = 3.670(2) Å; *Cg*2 is the centroid of N1/C1/N3/C2/C3/C4, Fig. S3†] and lone-pair (lp)···π interaction [C20–O4···*Cg*3^{vii} = 3.346(4) Å, θ = 87.4(3)°, *Cg*3 is the centroid of N4/C7/N6/C10/C9/C8, θ is the angle between the O, the ring centroid and the aromatic plane, Fig. S4†] act as a "glue" to reinforce the packing of the nets. (Symmetry code: (v) $-x$ + 3/2, y − 1/2, $-z$ + 3/2; (vi) $-x$ + 1, $-y$ + 1, $-z$ + 1; (vii) $-x$ + 3/2, y + 1/2, $-z$ + 3/2.)

3.2. Roles of the amino- and carboxyl-containing ligands

In this work, we selected amino-containing N-heterocyclic ligands instead of simple N-heterocyclic ligands based on following considerations: (i) their demonstrated ability to form very stable hydrogen-bonded arrays *via* their stereochemically associative amino groups,[15] (ii) established diverse metal binding patterns include the ring nitrogen atom[16a] or the exocyclic amino group,[16b] occasionally in equilibrium,[16c] and simultaneously both positions, either in a chelating or bridging fashion.[16d] Recently, our group found that the amino group can deprotonate to form –NH$^-$ in high pH environments (*ca.* 13) and exhibits rare μ_1- and μ_2-coordination fashions.[17] Herein, dmapym acts as a μ_2-bridge through heterocyclic nitrogens to link Ag(I) ions into low-dimensional coordination motifs and its amino group can be seen as an additional site for the binding of dicarboxylate anions to form hydrogen bonds which favor to the stabilization of the resultant networks. On the other hand, multidentate carboxylate ligands have been identified to be good candidates for building CPs owing to their diverse coordination modes.[18] In this system, we selected one flexible aliphatic and one rigid aromatic dicarboxylate as auxiliary ligands which extend the low-dimensional coordination motifs into high-dimensional networks. Although suc and bdc show the same coordination mode (μ_2-η^1:η^0:η^1:η^0) in **1** and **2**, they are different in size, length and geometry, as a result, giving two distinct interpenetrating structures. These results clearly demonstrate that the structural diversities of the complexes are undoubtedly associated with the auxiliary dicarboxylate-directed inclusion.

3.3. Syntheses and IR spectra

The syntheses of complexes **1** and **2** are carried out in the darkness to avoid photodecomposition, and are summarized in Scheme S1.† The formation of the products is not significantly affected by changes of the reaction mole ratio of organic ligands to metal ions and the resultant crystals are insoluble in water and common organic solvents. As is well known, the reactions of Ag(I) with multicarboxylates in aqueous solution often result in the formation of insoluble silver salts, presumably due to the fast coordination of the carboxylates to Ag(I) ions to form polymers.[19] Hence, properly lowering the reaction speed, such as by using ammoniacal conditions, may favor to the formation of crystalline products.[20] X-Ray powder diffraction measurements (Fig. S5†) and elemental analyses show that the pure phases of **1** and **2** have been obtained. The IR spectra of **1** and **2** (Fig. S6†) are fully consistent with their structural characteristics as determined by single-crystal X-ray diffraction. The IR spectra show the N–H asymmetric and symmetric stretching bands in the ranges of 3424–3318 and 3169–3157 cm^{-1}, respectively.[15b] The strong characteristic bands of carboxyl groups fall in the range of 1668–1562 cm^{-1} for the asymmetric vibrations and 1487–1381 cm^{-1} for symmetric vibrations, respectively. The absence of the characteristic bands at around ~1700 cm^{-1} are attributed to the carboxyl groups, indicating that the complete deprotonation of all carboxyl groups in **1** and **2** upon reaction with Ag(I) ions.[21]

3.4. Thermal properties

Thermogravimetric analysis (Fig. 5) showed that both **1** and **2** have three identifiable weight loss steps. For **1**, the first weight loss of 3.32% in the range of 20–125 °C corresponds to one H_2O

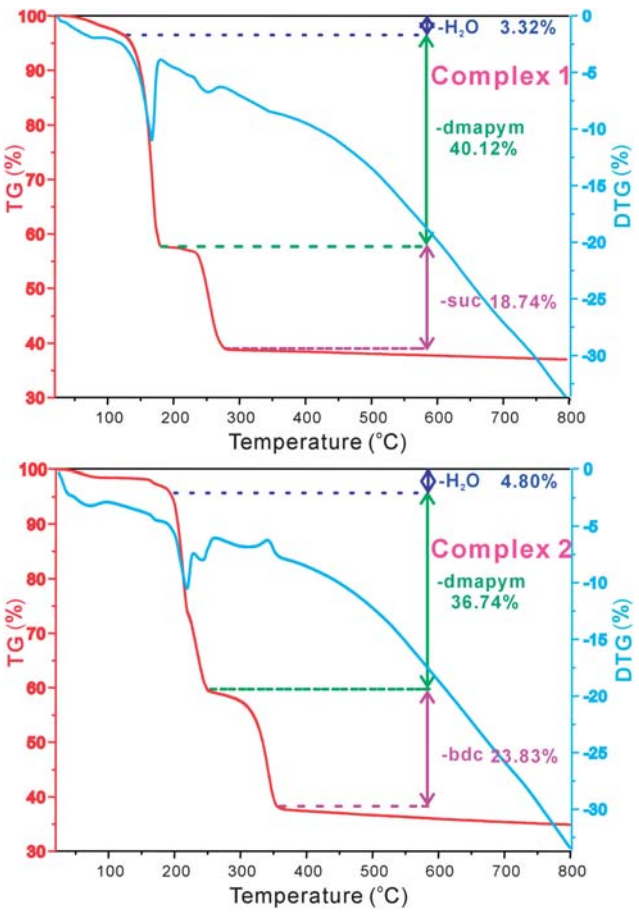

Fig. 5 TGA plots of complex **1** and **2**.

molecule per formula unit (calcd. 3.02%). The second weight loss of 40.12% between 125 and 180 °C is attributed to the loss of two dmapym ligands per formula unit (calcd. 41.33%) and one strong exothermic peak is observed at 172 °C. The loss of one suc ligand takes place at 232–282 °C (obsd 18.74%, calcd. 19.49%). For **2**, the initial weight loss of 4.80% from 20 to 192 °C, corresponds to the loss of two discrete water molecules per formula unit (calcd. 5.47%). The second weight loss of 36.74% between 192 and 249 °C is attributed to the loss of two dmapym ligands per formula unit (calcd. 37.38%). The loss of one bdc ligand takes place at 250–350 °C (obsd 23.83%, calcd. 24.92%).

3.5. Photoluminescence properties

The photoluminescent properties of the free ligands H_2suc, H_2bdc and complexes **1** and **2** have been investigated in the solid state at room temperature (Fig. 6). The free ligands H_2suc, H_2bdc and dmapym display luminescence with emission maxima at 420, 358 and 342 nm, respectively, upon excitation at 300 nm. It can be presumed that these peaks should be assigned to the $\pi^* \rightarrow n$ transitions for dicarboxylates and $\pi^* \rightarrow \pi$ transitions for dmapym, respectively. Intense emissions are observed at 369 nm (λ_{ex} = 320 nm) for **1** and 467 nm (λ_{ex} = 380 nm) for **2**, respectively. The photoluminescence of H_2suc is very weak compared to that of the dmapym, so the H_2suc almost have no contribution to the fluorescent emission of complex **1**.[22] Therefore, the emission band of **1** originates from the intraligand $\pi^* \rightarrow \pi$ transition of the N-donor ligands. When compared to the photoluminescence of the free dmapym, the emission band of **2** is red-shifted by 126 nm, which may come from the electronic transition between p orbitals (filled orbitals) of coordinated N atoms and 5s orbital (empty orbital) of Ag(I) ion, *i.e.*, ligand-to-metal charge transfer (LMCT), mixed with metal-centered (d–s/d–p) transitions.[23] The enhancement of luminescence of **1** and **2** is attributed to the ligand coordination to the metal center, which effectively increases the rigidity of the ligand and reduces the loss of energy by radiationless decay.

4. Conclusions

In summary, we used two kinds of simple ligands to constructed two interpenetrated networks, one presents an argentophilic interaction enhanced 2-crossing [2]-catenane motif formed between pairs of parallel interpenetrating 2D 4^4-**sql** nets and the other one is a 2D → 3D network showing the increase of dimensionality *via* interpenetration of the low-dimensional net. The geometries and flexibility of dicarboxylates influence the coordination environments of metal ions and arrangement of ligands and thus result in two distinct interpenetrating networks.

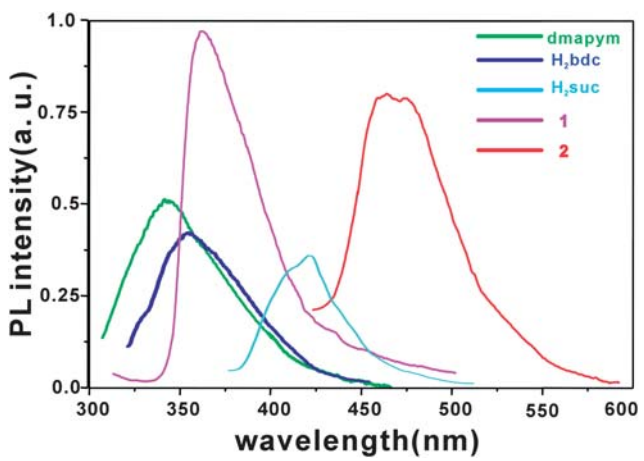

Fig. 6 Photoluminescences of ligands and complexes **1** and **2**.

Acknowledgements

This work was financially supported by the National Natural Science Foundation of China (No. 20721001), 973 Project (Grant 2007CB815301) from MSTC.

Notes and references

1 (*a*) J. R. Li, R. J. Kuppler and H. C. Zhou, *Chem. Soc. Rev.*, 2009, **38**, 1477; (*b*) X. C. Huang, Y. Y. Lin, J. P. Zhang and X. M. Chen, *Angew. Chem., Int. Ed.*, 2006, **45**, 1557; (*c*) L. J. Murray, M. Dincă and J. R. Long, *Chem. Soc. Rev.*, 2009, **38**, 1294; (*d*) J. Lee, O. K. Farha, J. Roberts, K. A. Scheidt, S. T. Nguyen and J. T. Hupp, *Chem. Soc. Rev.*, 2009, **38**, 1450; (*e*) Y. Ma, Z. B. Han, Y. K. He and L. G. Yang, *Chem. Commun.*, 2007, 4170; (*f*) M. Kurmoo, *Chem. Soc. Rev.*, 2009, **38**, 1353.

2 (*a*) X. H. Bu, M. L. Tong, H. C. Chang, S. Kitagawa and S. R. Batten, *Angew. Chem., Int. Ed.*, 2004, **43**, 192; (*b*) C. Y. Su, A. M. Goforth, M. D. Smith and H. C. zur. Loye, *Chem. Commun.*, 2004, 2158; (*c*) X. L. Wang, C. Qin, E. B. Wang, Y. G. Li, Z. M. Su, L. Xu and L. Carlucci, *Angew. Chem., Int. Ed.*, 2005, **44**, 5824; (*d*) X. L. Zhang, C. P. Guo, Q. Y. Yang, W. Wang, W. S. Liu, B. S. Kang and C. Y. Su, *Chem. Commun.*, 2007, 4242; (*e*) L. Dobrzanska, H. G. Raubenheimer and L. J. Barbour, *Chem. Commun.*, 2005, 5050.

3 (*a*) S. R. Batten and R. Robson, *Angew. Chem., Int. Ed.*, 1998, **37**, 1460; (*b*) S. R. Batten, *CrystEngComm*, 2001, **3**, 67.

4 (*a*) O. M. Yaghi, G. Li and H. Li, *Nature*, 1995, **378**, 703; (*b*) L. R. MacGillivray, R. H. Groeneman and J. L. Atwood, *J. Am. Chem. Soc.*, 1998, **120**, 2676.

5 M. L. Tong, X. M. Chen, B. H. Ye and L. N. Ji, *Angew. Chem., Int. Ed.*, 1999, **38**, 2237.

6 (*a*) J.-Q. Liu, Y.-Y. Wang, L.-F. Ma, G.-L. Wen, Q.-Z. Shi, S. R. Batten and D. M. Proserpio, *CrystEngComm*, 2008, **10**, 1123; (*b*) K. A. Hirsch, S. R. Wilson and J. S. Moore, *Inorg. Chem.*, 1997, **36**, 2960; (*c*) Y. Kang, J. Zhang, Y.-Y. Qin, Z.-J. Li and Y.-G. Yao, *J. Mol. Struct.*, 2007, **827**, 126; (*d*) L. Carlucci, G. Ciani, D. M. Proserpio and S. Rizzato, *CrystEngComm*, 2002, **4**, 413; (*e*) O. D. Friedrichs, M. O'Keeffe and O. M. Yaghi, *Solid State Sci.*, 2003, **5**, 73; (*f*) Y.-B. Dong, P. Wang, R.-Q. Huang and M. D. Smith, *Inorg. Chem.*, 2004, **43**, 4727; (*g*) T. Soma and T. Iwamoto, *Chem. Lett.*, 1994, 821; (*h*) S. R. Batten, B. F. Hoskins and R. Robson, *Chem.–Eur. J.*, 2000, **6**, 156; (*i*) L. Carlucci, G. Ciani, D. M. Proserpio and S. Rizzato, *CrystEngComm*, 2002, **4**, 413; (*j*) L. Carlucci, G. Ciani, D. M. Proserpio and S. Rizzato, *CrystEngComm*, 2002, **4**, 121; (*k*) M. Du, X. J. Jiang and X. J. Zhao, *Chem. Commun.*, 2005, 5521.

7 F. Q. Liu and T. D. Tilley, *Inorg. Chem.*, 1997, **36**, 5090.

8 (*a*) S. R. Batten, A. R. Harris, P. Jensen, K. S. Murray and A. Ziebell, *J. Chem. Soc., Dalton Trans.*, 2000, 3829; (*b*) L. Carlucci, G. Ciani, D. M. Proserpio and S. Rizzato, *Chem. Commun.*, 2000, 1319; (*c*) S. M.-F. Lo, S. S.-Y. Chui, L.-Y. Shek, Z. Lin, X. X. Zhang, G. Wen and I. D. Williams, *J. Am. Chem. Soc.*, 2000, **122**, 6293; (*d*) E.-Q. Gao, S.-Q. Bai, Z.-M. Wang and C.-H. Yan, *Dalton Trans.*, 2003, 1759; (*e*) D. J. Chesnut, A. Kusnetzow, R. Birge and J. Zubieta, *Inorg. Chem.*, 1999, **38**, 5484; (*f*) Q.-Y. Yang, S.-R. Zheng, R. Yang, M. Pan, R. Cao and C.-Y. Su, *CrystEngComm*, 2009, **11**, 680; (*g*) L. Carlucci, G. Ciani, P. Macchi, D. M. Proserpio and S. Rizzato, *Chem.–Eur. J.*, 1999, **5**, 237.

9 (*a*) D. Sun, G. G. Luo, N. Zhang, J. H. Chen, R. B. Huang, L. R. Lin and L. S. Zheng, *Polyhedron*, 2009, **28**, 2983; (*b*) D. Sun, G. G. Luo, N. Zhang, Z. H. Wei, C. F. Yang, Q. J. Xu, R. B. Huang and L. S. Zheng, *J. Mol. Struct.*, 2010, **967**, 147; (*c*) D. Sun, N. Zhang,

G. G. Luo, Q. J. Xu, R. B. Huang and L. S. Zheng, *Polyhedron*, 2010, **29**, 1842; (*d*) D. Sun, N. Zhang, G. G. Luo, Q. J. Xu, R. B. Huang and L. S. Zheng, *J. Organomet. Chem.*, 2010, **695**, 1598.
10 (*a*) G. M. Sheldrick, *SHELXS 97: Program for Crystal Structure Solution*, University of Göttingen, Göttingen, Germany, 1997; (*b*) G. M. Sheldrick, *SHELXL 97: Program for Crystal Structure refinement*, University of Göttingen, Göttingen, Germany, 1997.
11 L. Yang, D. R. Powell and R. P. Houser, *Dalton Trans.*, 2007, 955.
12 (*a*) D. Sun, G. G. Luo, Q. J. Xu, N. Zhang, Y. C. Jin, H. X. Zhao, R. B. Huang and L. S. Zheng, *Inorg. Chem. Commun.*, 2009, **12**, 782; (*b*) D. Sun, G. G. Luo, N. Zhang, Q. J. Xu, R. B. Huang and L. S. Zheng, *Polyhedron*, 2010, **29**, 1243; (*c*) I. A. Gural'skiy, D. Escudero, A. Frontera, P. V. Solntsev, E. B. Rusanov, A. N. Chernega, H. Krautscheid and K. V. Domasevitch, *Dalton Trans.*, 2009, 2856; (*d*) K. V. Domasevitch, P. V. Solntsev, I. A. Gural'skiy, H. Krautscheid, E. B. Rusanov, A. N. Chernega and J. A. K. Howard, *Dalton Trans.*, 2007, 3893; (*e*) A. S. Degtyarenko, P. V. Solntsev, H. Krautscheid, E. B. Rusanov, A. N. Chernega and K. V Domasevitch, *New J. Chem.*, 2008, **32**, 1910; (*f*) I. A. Gural'skiy, P. V. Solntsev, H. Krautscheid and K. V. Domasevitch, *Chem. Commun.*, 2006, 4808.
13 (*a*) V. A. Blatov, M. O'Keeffe and D. M. Proserpio, *CrystEngComm*, 2010, **12**, 44; (*b*) I. A. Baburin, V. A. Blatov, L. Carlucci, G. Cianib and D. M. Proserpio, *CrystEngComm*, 2008, **10**, 1822; (*c*) I. A. Baburin, V. A. Blatov, L. Carlucci, G. Cianib and D. M. Proserpio, *Cryst. Growth Des.*, 2008, **8**, 519.
14 J. Bernstein, R. E. Davis, L. Shimoni and N.-L. Chang, *Angew. Chem., Int. Ed. Engl.*, 1995, **34**, 1555.
15 (*a*) C.-Y. Lin, Z.-K. Chan, C.-W. Yeh, C.-J. Wu, J.-D. Chen and J.-C. Wang, *CrystEngComm*, 2006, **8**, 841; (*b*) Y.-H. Wang, K.-L. Chu, H.-C. Chen, C.-W. Yeh, Z.-K. Chan, M.-C. Suen and J.-D. Chen, *CrystEngComm*, 2006, **8**, 84; (*c*) K. V. Domasevitch, I. Boldog, E. B. Rusanov, J. Hunger, S. Blaurock, M. Schröder and J. Sieler, *Z. Anorg. Allg. Chem.*, 2005, **631**, 1095.
16 (*a*) O. Krizanovic, M. Sabat, R. Beyerle-Pfnür and B. Lippert, *J. Am. Chem. Soc.*, 1993, **115**, 5538; (*b*) W. Z. Shen, B. Costisella and B. Lippert, *Dalton Trans.*, 2007, 851; (*c*) L. G. Marzilli, M. F. Summers, E. Zangrando, N. Bresciani-Pahor and L. Randaccio, *J. Am. Chem. Soc.*, 1986, **108**, 4830; (*d*) A. Spannenberg, P. Arndt and R. Kempe, *Angew. Chem., Int. Ed.*, 1998, **37**, 832.
17 (*a*) D. Sun, G. G. Luo, N. Zhang, Q. J. Xu, Z. H. Wei, C. F. Yang, L. R. Lin, R. B. Huang and L. S. Zheng, *Bull. Chem. Soc. Jpn.*, 2010, **83**, 173; (*b*) D. Sun, G. G. Luo, N. Zhang, Q. J. Xu, C. F. Yang, Z. H. Wei, Y. C. Jin, L. R. Lin, R. B. Huang and L. S. Zheng, *Inorg. Chem. Commun.*, 2010, **13**, 290.
18 (*a*) L. Hou, J. P. Zhang, X. M. Chen and S. W. Ng, *Chem. Commun.*, 2008, 4019; (*b*) S. Q. Ma and H. C. Zhou, *J. Am. Chem. Soc.*, 2006, **128**, 11734; (*c*) B. Chen, M. Eddaoudi, S. T. Hyde, M. O'Keeffe and O. M. Yaghi, *Science*, 2001, **291**, 1021; (*d*) G. Férey, C. Mellot-Draznieks, C. Serre and F. Millange, *Acc. Chem. Res.*, 2005, **38**, 217; (*e*) K. Koh, A. G. Wong-Foy and A. J. Matzger, *Angew. Chem., Int. Ed.*, 2008, **47**, 677.
19 D. F. Sun, R. Cao, W. H. Bi, M. C. Hong and Y. L. Chang, *Inorg. Chim. Acta*, 2004, **357**, 991.
20 D. Sun, G. G. Luo, N. Zhang, Z. H. Wei, C. F. Yang, Q. J. Xu, R. B. Huang and L. S. Zheng, *Chem. Lett.*, 2010, **39**, 190.
21 (*a*) K. Nakamoto, *Infrared and Raman Spectra of Inorganic and Coordination Compounds*, John Wiley & Sons, New York, 1986; (*b*) L. J. Bellamy, *The Infrared Spectra of Complex Molecules*, Wiley, New York, 1958.
22 (*a*) H. Schmidbaur, *Chem. Soc. Rev.*, 1995, **24**, 391; (*b*) V. W. W. Yam, E. C. C. Cheng and K. K. Cheung, *Angew. Chem., Int. Ed.*, 1999, **38**, 197; (*c*) V. W. W. Yam, K. K. W. Lo, W. K. M. Fung and C. R. Wang, *Coord. Chem. Rev.*, 1998, **171**, 17; (*d*) V. W. W. Yam and K. K. W. Lo, *Chem. Soc. Rev.*, 1999, **28**, 323; (*e*) W. Chen, J. Y. Wang, C. Chen, Q. Yue, H. M. Yuan, J. S. Chen and S. N. Wang, *Inorg. Chem.*, 2003, **42**, 944.
23 G. Accorsi, A. Listorti, K. Yoosaf and N. Armaroli, *Chem. Soc. Rev.*, 2009, **38**, 1690.